

Supplementary information for Determination of molecular hydration in solution via changes in magnetic anisotropy

Marcus J. Giansiracusa,¹ Michele Vonci,¹ Yasmin L. Whyatt,¹ Carys Williams,¹ Kevin Mason,² David Parker,^{2,*} Eric J. L. McInnes^{1,*} and Nicholas F. Chilton^{1,*}

¹ Department of Chemistry, The University of Manchester, Oxford Road, Manchester, M13 9PL, UK

² Department of Chemistry, Durham University, South Road, Durham, DH1 3LE, UK

Experimental methods

Proton and ³¹P NMR spectra were recorded in commercially-available deuterated solvents on a Varian Mercury-400 (¹H at 399.960 MHz and ³¹P at 161.943 MHz), or a Varian VNMRA-700 (¹H at 699.731 MHz, ³¹P at 283.256 MHz) spectrometer. All chemical shifts are given in ppm and coupling constants are reported in Hz. Where required, the operating temperature of the spectrometer was measured with the aid of an internal calibration solution of ethylene glycol.

Low resolution electrospray mass spectra were obtained on a TQD mass spectrometer, operating in positive or negative ion mode, equipped with an Acquity UPLC, an electrospray ion source and an Acquity photodiode array detector (Waters Ltd, UK). High resolution electrospray mass spectra were recorded on a LCT Premier XE mass spectrometer or a QTOF Premier mass spectrometer, both equipped with an Acquity UPLC, a lock-mass electrospray ion source and an Acquity photodiode array detector (Waters Ltd, UK).

Reverse phase HPLC was performed at 295 K using a Shimadzu system consisting of a Degassing Unit (DGU-20A5R), a Prominence Preparative Liquid Chromatograph (LC-20AP), a Prominence UV/Vis Detector (SPD-20A) and a Communications Bus Module (CBM-20A). An XBridge C18 19 x 100 mm, i.d. 5 μM column was used to purify the erbium(III) complexes on a preparative scale (flow rate 17 mL/min) and an XBridge C18 column, 4.6 x 100 mm, i.d. 5 μM (flow rate 2 mL/min) was used for analytical scale purifications. A gradient elution with a solvent system composed of H₂O + 0.1% HCOOH/ MeOH + 0.1% HCOOH was performed for a total run time of 17 min. The separation details are reported below (Table S1). Fraction collection was performed manually.

Table S1. Preparative HPLC Procedure (flow rate = 17 mL/min; Solvent A = H₂O + 0.1% formic acid; Solvent B = MeOH + 0.1% formic acid).

| Time (min) | Solvent A (%) | Solvent B(%) |
|------------|---------------|--------------|
| 0 | 90 | 10 |
| 3 | 90 | 10 |
| 13 | 0 | 100 |
| 16 | 0 | 100 |
| 17 | 90 | 10 |

EPR spectroscopy was performed on powder samples of **1**_{solid} and **2**_{solid} in quartz EPR tubes, and frozen solutions (H₂O:glycerol 8:2) of **1**_{solution} and **2**_{solution} in silica capillaries, at Q-band frequency (ca. 34 GHz) with a Bruker EMX spectrometer using liquid helium cooling.

Semi-empirical optimisations were performed on hydrated cluster models of **1** and **2** using MOPAC with the PM6 method,^{3,4} where either the Er^{III} complex was frozen or not. Subsequent DFT optimisations of these hydrated cluster models, where Er was replaced with Y, were performed using Gaussian 09d,⁵ the M06-2X functional,⁶ the cc-pVDZ basis set⁷ for all non-metal atoms, the Stuttgart RSC 1997 ECP⁸ for Y, the SMD continuum solvent model,⁹ and GD3¹⁰ dispersion corrections. Due to the many degrees of freedom and shallow potential energy surface, it was not possible to fully converge the DFT optimisations; residual forces were on the order of $2.0 \times 10^{-2} \text{ eV \AA}^{-3}$ compared to the standard convergence threshold of $1.5 \times 10^{-2} \text{ eV \AA}^{-3}$. CASSCF-SO calculations were performed using OpenMolcas¹¹ where the active space comprised eleven 4f electrons in seven 4f orbitals of Er^{III} for 35 quartet and 112 doublet roots. Basis sets were taken from the ANO-RCC library where Er atom had VTZP quality, coordinated O and N atoms had VDZP quality, remaining atoms had VDZ quality and surrounding waters had MB quality.¹²⁻¹⁴ The two electron integrals were decomposed using the Cholesky method with a threshold of 10^{-8} to save computational resources.

Synthesis of **1** and **2**

The syntheses of *tert*-Butyl-2,2',2''-(10-((5-*tert*-butylpyridin-2-yl)methyl)-1,4,7,10-tetraazacyclododecane-1,4,7-triyl)triacetate (L¹) and ethyl ({4-[(5-*tert*-butylpyridin-2-yl)methyl]-7,10-di[[ethoxy(methyl)phosphoryl]methyl]-1,4,7,10-tetraazacyclododecan-1-yl)methyl}(methyl)phosphinate (L²) are given in references 1 and 2.

[ErL¹] (**1**):

tert-Butyl-2,2',2''-(10-((5-*tert*-butylpyridin-2-yl)methyl)-1,4,7,10-tetraazacyclododecane-1,4,7-triyl)triacetate (100 mg, 0.15 mmol) was dissolved in CH₂Cl₂ (1 mL) and to this was added TFA (1 mL). The resulting mixture was stirred at room temperature for 18 h. Excess CH₂Cl₂ and TFA were removed under reduced pressure and the resulting yellow residue was repeatedly washed with CH₂Cl₂ (3 x 1 mL). Deprotection was monitored by ESI-LRMS (+) (*m/z* 494.2 [M+H]⁺; ESI-HRMS (+) calc. for [C₂₄H₄₀N₅O₆]⁺ 494.2979, found 494.2963) and complete loss of the *t*-butyl groups was confirmed by ¹H NMR spectroscopy. The residue was dissolved in H₂O (2 mL) and the pH adjusted to 5.5. To this solution was added ErCl₃.6H₂O (63mg, 0.17 mmol), and the resulting mixture was stirred at 70 ° C for 18 h, before the solvent was removed under reduced pressure. The resulting yellow solid was purified by reverse-phase HPLC (10-100% MeOH in H₂O over 10 min; *t_R* = 8.9 min) to yield a white solid (29 mg, 29%). ¹H NMR (400 MHz, D₂O) δ 7.0 (C(CH₃)₃); ESI-LRMS (+) *m/z* 657.1 [MH]⁺; ESI-HRMS (+) calc. for [C₂₄H₃₇N₅O₆¹⁶⁶Er]⁺ 657.2047, found 657.2045.

[ErL²] (**2**):

Ethyl ({4-[(5-*tert*-butylpyridin-2-yl)methyl]-7,10-di[[ethoxy(methyl)phosphoryl]methyl]-1,4,7,10-tetraazacyclododecan-1-yl)methyl}(methyl)phosphinate (45 mg, 0.065 mmol) was dissolved in aqueous HCl (6M, 2 mL) and stirred at 70 ° C for 18 h. Complete ester hydrolysis was confirmed by ³¹P NMR spectroscopy ((162 MHz, D₂O) δ 37.0, 34.4, 30.6), before the solvent was removed under reduced pressure. The resulting yellow oil was dissolved in H₂O (2 mL) and the pH of the solution adjusted to 5.5 using aqueous sodium hydroxide solution. ErCl₃.6H₂O (37 mg, 0.098 mmol), was added and the solution was stirred at 70 ° C for 18 h before solvent was removed under reduced pressure. The resulting pale yellow solid was purified by reverse-phase HPLC (10-100% MeOH in H₂O over 10 min; *t_R* = 8.6 min) to yield a colourless solid (16 mg, 32%). ¹H NMR (400MHz, D₂O) δ 38.3 (C(CH₃)₃ major), 40.1 (C(CH₃)₃ minor); ESI-LRMS (+) *m/z* 758.9[M+H]⁺; ESI-HRMS (+) calc. for [C₂₄H₄₆N₅O₆P₃¹⁶⁴Er]⁺ 757.1953, found 757.1962.

Table S2. Electronic states for non-hydrated crystalline **1- Δ - $\delta\delta\delta\delta$** (using X-Ray structure of [YbL¹]) calculated by CASSCF-SO.

| Energy (cm ⁻¹) | <i>g</i> ₁ | <i>g</i> ₂ | <i>g</i> ₃ |
|----------------------------|-----------------------|-----------------------|-----------------------|
| 0.0 | 1.32 | 2.39 | 14.26 |
| 60.8 | 1.00 | 1.91 | 15.22 |
| 106.4 | 2.52 | 4.74 | 8.41 |
| 157.4 | 0.17 | 2.36 | 12.03 |
| 295.8 | 1.09 | 1.17 | 14.36 |
| 379.1 | 2.78 | 5.91 | 7.81 |
| 425.8 | 2.37 | 4.82 | 8.94 |
| 464.5 | 1.46 | 2.56 | 14.31 |

Table S3. Electronic states for non-hydrated crystalline **2- Δ - $\delta\delta\delta\delta$** (using X-Ray structure of [YbL²]) calculated by CASSCF-SO.

| Energy (cm ⁻¹) | <i>g</i> ₁ | <i>g</i> ₂ | <i>g</i> ₃ |
|----------------------------|-----------------------|-----------------------|-----------------------|
| 0.0 | 0.91 | 1.77 | 15.19 |
| 45.6 | 2.09 | 3.05 | 13.92 |
| 90.8 | 1.24 | 4.06 | 8.49 |
| 120.6 | 0.52 | 3.29 | 12.12 |
| 222.3 | 0.04 | 0.90 | 15.22 |
| 320.6 | 2.08 | 4.37 | 9.95 |
| 357.4 | 1.56 | 4.48 | 10.78 |
| 380.4 | 1.21 | 1.87 | 15.20 |

Table S4. Electronic states for non-hydrated crystalline **2- Λ - $\lambda\lambda\lambda\lambda$** (using X-Ray structure of [YbL²]) calculated by CASSCF-SO.

| Energy (cm ⁻¹) | <i>g</i> ₁ | <i>g</i> ₂ | <i>g</i> ₃ |
|----------------------------|-----------------------|-----------------------|-----------------------|
| 0.0 | 0.84 | 1.59 | 15.24 |
| 44.0 | 1.91 | 2.64 | 14.37 |
| 88.2 | 1.89 | 4.81 | 8.56 |
| 122.2 | 0.66 | 2.73 | 12.47 |
| 221.4 | 0.19 | 0.93 | 15.23 |
| 314.4 | 0.77 | 1.92 | 13.01 |
| 365.5 | 0.23 | 2.36 | 13.76 |
| 387.2 | 0.92 | 1.55 | 15.68 |

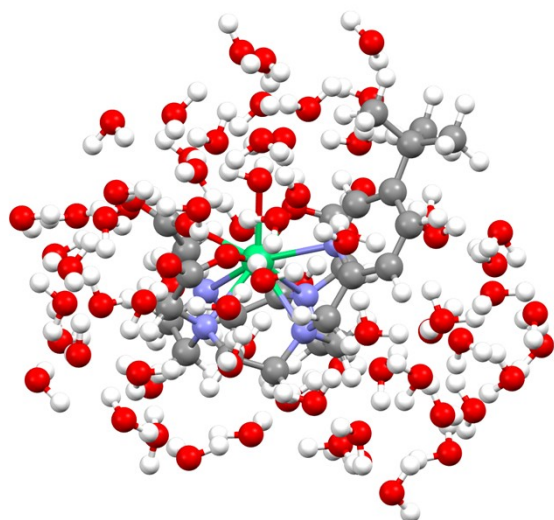


Figure S1. Optimised structure of **1A_{solution}**.

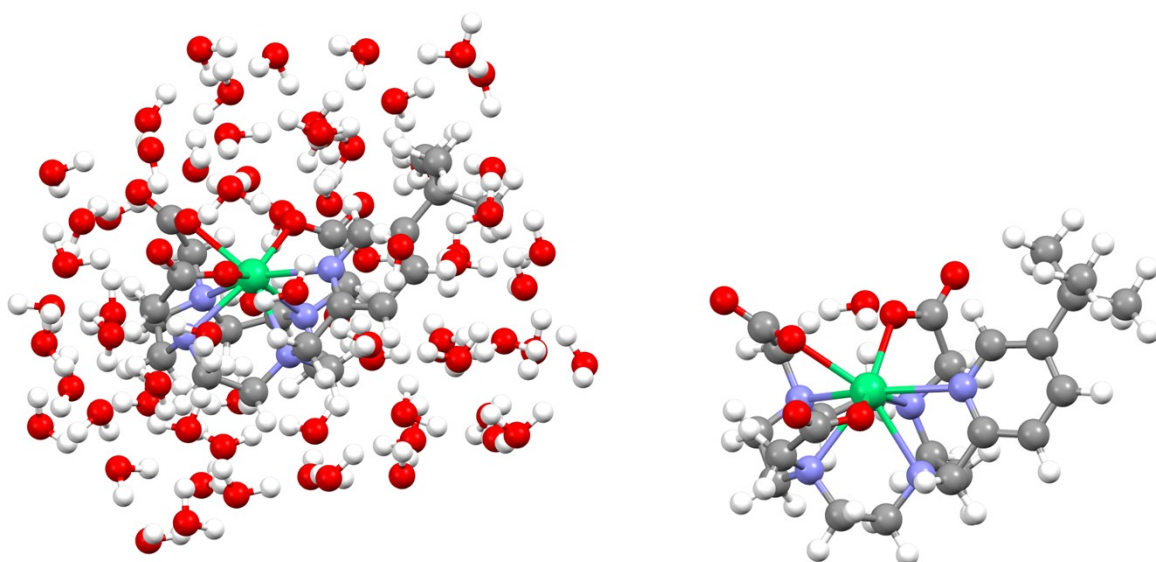


Figure S2. Optimised structure of **1B_{solution}**. Left: full structure; right: coordination complex only.

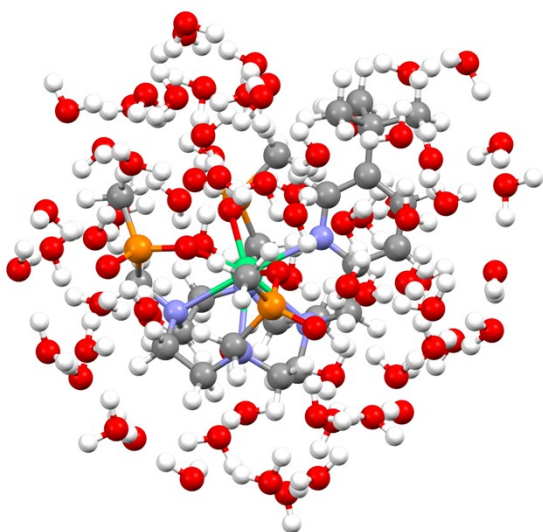


Figure S3. Optimised structure of **2A_{solution}**.

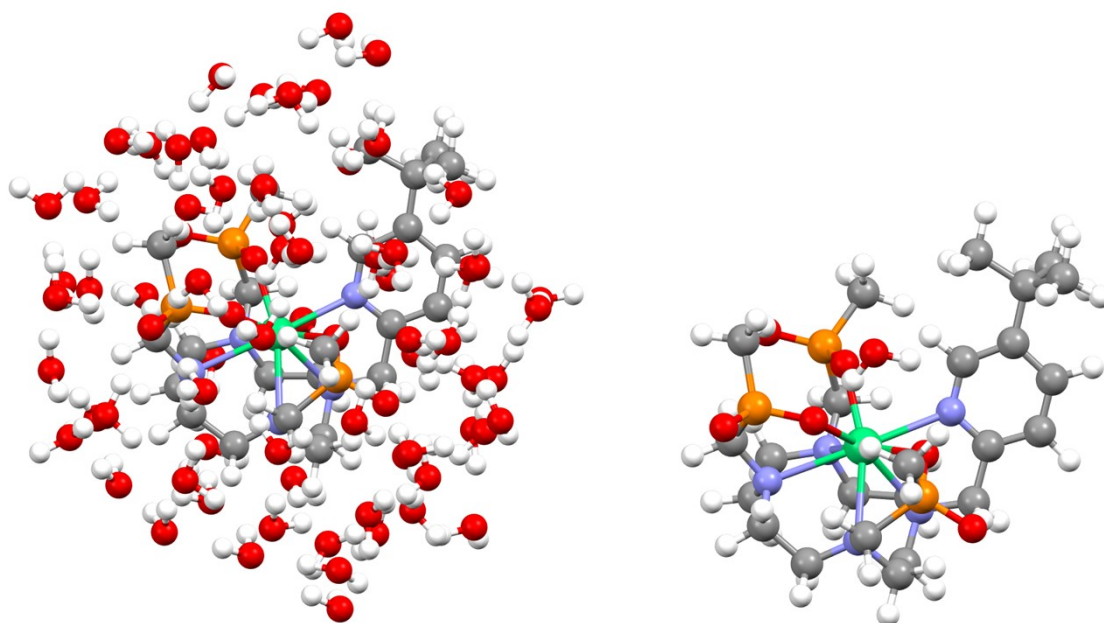


Figure S4. Optimised structure of $2\mathbf{B}_{\text{solution}}$. Left: full structure; right: coordination complex only.

Table S5. Electronic states for DFT-optimised $1\mathbf{A}_{\text{solution}}$ calculated by CASSCF-SO.

| Energy (cm^{-1}) | g_1 | g_2 | g_3 |
|-----------------------------|-------|-------|-------|
| 0.0 | 1.94 | 5.46 | 11.60 |
| 43.9 | 2.70 | 3.48 | 5.52 |
| 74.2 | 0.02 | 4.37 | 9.14 |
| 110.2 | 1.87 | 3.07 | 9.63 |
| 163.9 | 0.11 | 2.98 | 10.86 |
| 223.0 | 0.19 | 3.56 | 11.39 |
| 259.2 | 2.31 | 3.50 | 10.84 |
| 305.0 | 0.90 | 1.32 | 14.31 |

Table S6. Electronic states for DFT-optimised $1\mathbf{B}_{\text{solution}}$ calculated by CASSCF-SO.

| Energy (cm^{-1}) | g_1 | g_2 | g_3 |
|-----------------------------|-------|-------|-------|
| 0.0 | 0.93 | 5.77 | 11.15 |
| 26.9 | 1.23 | 3.62 | 12.55 |
| 66.5 | 3.64 | 5.48 | 9.51 |
| 109.6 | 0.15 | 1.18 | 11.83 |
| 211.0 | 1.40 | 2.84 | 10.36 |
| 246.3 | 0.05 | 6.17 | 9.99 |
| 275.1 | 2.90 | 3.61 | 10.50 |
| 335.5 | 0.60 | 0.79 | 15.63 |

Table S7. Electronic states for DFT-optimised **2A_{solution}** calculated by CASSCF-SO.

| Energy (cm ⁻¹) | <i>g</i> ₁ | <i>g</i> ₂ | <i>g</i> ₃ |
|----------------------------|-----------------------|-----------------------|-----------------------|
| 0.0 | 0.29 | 0.71 | 16.17 |
| 28.8 | 1.02 | 1.36 | 16.13 |
| 88.0 | 3.32 | 6.28 | 7.40 |
| 134.7 | 1.09 | 3.11 | 11.89 |
| 247.2 | 1.41 | 2.25 | 13.61 |
| 283.3 | 0.15 | 3.78 | 9.64 |
| 321.8 | 1.30 | 3.29 | 12.01 |
| 347.6 | 1.35 | 1.73 | 14.56 |

Table S8. Electronic states for DFT-optimised **2B_{solution}** calculated by CASSCF-SO.

| Energy (cm ⁻¹) | <i>g</i> ₁ | <i>g</i> ₂ | <i>g</i> ₃ |
|----------------------------|-----------------------|-----------------------|-----------------------|
| 0.0 | 0.63 | 3.11 | 13.37 |
| 18.6 | 1.43 | 1.81 | 15.62 |
| 76.0 | 2.24 | 4.57 | 7.43 |
| 106.6 | 1.48 | 4.47 | 11.76 |
| 236.7 | 1.41 | 2.33 | 13.24 |
| 276.2 | 3.02 | 4.57 | 7.96 |
| 310.6 | 1.88 | 4.92 | 10.99 |
| 353.9 | 0.51 | 0.53 | 16.85 |

References

- 1 A. M. Funk, K.-L. N. A. Finney, P. Harvey, A. M. Kenwright, E. R. Neil, N. J. Rogers, P. Kanthi Senanayake and D. Parker, *Chem Sci*, 2015, **6**, 1655–1662.
- 2 K. Mason, N. J. Rogers, E. A. Suturina, I. Kuprov, J. A. Aguilar, A. S. Batsanov, D. S. Yufit and D. Parker, *Inorg. Chem.*, 2017, **56**, 4028–4038.
- 3 J. J. P. Stewart, .
- 4 J. J. P. Stewart, *J. Mol. Model.*, 2007, **13**, 1173–1213.
- 5 M. J. Frisch, G. W. Trucks, H. B. Schlegel, G. E. Scuseria, M. A. Robb, J. R. Cheeseman, G. Scalmani, V. Barone, B. Mennucci, G. A. Petersson, H. Nakatsuji, M. Caricato, X. Li, H. P. Hratchian, A. F. Izmaylov, J. Bloino, G. Zheng, J. L. Sonnenberg, M. Hada, M. Ehara, K. Toyota, R. Fukuda, J. Hasegawa, M. Ishida, T. Nakajima, Y. Honda, O. Kitao, H. Nakai, T. Vreven, J. A. Montgomery Jr., J. E. Peralta, F. Ogliaro, M. Bearpark, J. J. Heyd, E. Brothers, K. N. Kudin, V. N. Staroverov, T. Keith, R. Kobayashi, J. Normand, K. Raghavachari, A. Rendell, J. C. Burant, S. S. Iyengar, J. Tomasi, M. Cossi, N. Rega, J. M. Millam, M. Klene, J. E. Knox, J. B. Cross, V. Bakken, C. Adamo, J. Jaramillo, R. Gomperts, R. E. Stratmann, O. Yazyev, A. J. Austin, R. Cammi, C. Pomelli, J. W. Ochterski, R. L. Martin, K. Morokuma, V. G. Zakrzewski, G. A. Voth, P. Salvador, J. J. Dannenberg, S. Dapprich, A. D. Daniels, Ö. Farkas, J. B. Foresman, J. V. Ortiz, J. Cioslowski and D. J. Fox, .
- 6 Y. Zhao and D. G. Truhlar, *Theor. Chem. Acc.*, 2008, **120**, 215–241.
- 7 T. H. Dunning, *J. Chem. Phys.*, 1989, **90**, 1007–1023.
- 8 M. Dolg, H. Stoll, H. Preuss and R. M. Pitzer, *J. Phys. Chem.*, 1993, **97**, 5852–5859.

- 9 A. V. Marenich, C. J. Cramer and D. G. Truhlar, *J. Phys. Chem. B*, 2009, **113**, 6378–6396.
- 10S. Grimme, J. Antony, S. Ehrlich and H. Krieg, *J. Chem. Phys.*, 2010, **132**, 154104.
- 11I. Fdez. Galván, M. Vacher, A. Alavi, C. Angeli, F. Aquilante, J. Autschbach, J. J. Bao, S. I. Bokarev, N. A. Bogdanov, R. K. Carlson, L. F. Chibotaru, J. Creutzberg, N. Dattani, M. G. Delcey, S. S. Dong, A. Dreuw, L. Freitag, L. M. Frutos, L. Gagliardi, F. Gendron, A. Giussani, L. González, G. Grell, M. Guo, C. E. Hoyer, M. Johansson, S. Keller, S. Knecht, G. Kovačević, E. Källman, G. Li Manni, M. Lundberg, Y. Ma, S. Mai, J. P. Malhado, P. Å. Malmqvist, P. Marquetand, S. A. Mewes, J. Norell, M. Olivucci, M. Oppel, Q. M. Phung, K. Pierloot, F. Plasser, M. Reiher, A. M. Sand, I. Schapiro, P. Sharma, C. J. Stein, L. K. Sørensen, D. G. Truhlar, M. Ugandi, L. Ungur, A. Valentini, S. Vancoillie, V. Veryazov, O. Weser, T. A. Wesolowski, P.-O. Widmark, S. Wouters, A. Zech, J. P. Zobel and R. Lindh, *J. Chem. Theory Comput.*, 2019, **15**, 5925–5964.
- 12B. O. Roos, R. Lindh, P.-Å. Malmqvist, V. Veryazov and P.-O. Widmark, *Chem. Phys. Lett.*, 2005, **409**, 295–299.
- 13B. O. Roos, R. Lindh, P.-Å. Malmqvist, V. Veryazov and P.-O. Widmark, *J. Phys. Chem. A*, 2005, **109**, 6575–6579.
- 14B. O. Roos, R. Lindh, P.-Å. Malmqvist, V. Veryazov and P.-O. Widmark, *J. Phys. Chem. A*, 2004, **108**, 2851–2858.